JOURNAL OF GEOPHYSICAL RESEARCH, VOL. 111, B10403, doi:10.1029/2006JB004405, 2006

Hydrogeological investigations at the Membach station, Belgium, and application to correct long periodic gravity variations

M. Van Camp,[1] M. Vanclooster,[2] O. Crommen,[3] T. Petermans,[1] K. Verbeeck,[1] B. Meurers,[4] T. van Dam,[5] and A. Dassargues[3]

Received 21 March 2006; revised 8 May 2006; accepted 6 July 2006; published 20 October 2006.

[1] A comprehensive hydrogeological investigation regarding the influence of variations in local and regional water mass on superconducting gravity measurements is presented for observations taken near the geodynamic station of Membach, Belgium. Applying a regional water storage model, the gravity contribution due to the elastic deformation of the Earth was derived. In addition, the Newtonian gravity effect induced by the local water mass variations was calculated, using soil moisture observations taken at the ground surface (about 48 m above the gravimeters). The computation of the gravimetric effect is based on a digital elevation model with spatially discretized rectangular prisms. The obtained results are compared with the observations of a superconducting gravimeter (SG). We find that the seasonal variations can be reasonably well predicted with the regional water storage model and the local Newtonian effects. Shorter-period effects depend on the local changes in hydrology. This result shows the sensitivity of SG observations to very local water storage changes.

Citation: Van Camp, M., M. Vanclooster, O. Crommen, T. Petermans, K. Verbeeck, B. Meurers, T. van Dam, and A. Dassargues (2006), Hydrogeological investigations at the Membach station, Belgium, and application to correct long periodic gravity variations, *J. Geophys. Res.*, *111*, B10403, doi:10.1029/2006JB004405.

1. Introduction

[2] Stable gravity observations over long periods can be a useful tool for understanding geodynamic changes related to Earth structure [*Hinderer and Crossley*, 2000], tectonics [*Francis et al.*, 2004], postglacial rebound [*Williams et al.*, 2001; *Lambert et al.*, 2001] and natural as well as anthropogenic subsidence [*Zerbini et al.*, 2001, 2005]. However, gravity is also affected by changes in environmental surface mass. To obtain a reliable estimate of the geodynamic signal, corrections for environmental mass changes are routinely applied to the gravity time series. In the past, the focus was on the effects of atmospheric mass movements; for an excellent review of this problem please refer to *Spratt* [1982], *Merriam* [1992], and *Boy et al.* [2002], who applied routine corrections to continuous superconducting gravimeter time series.

[3] The influence of regional and local water storage variations on gravity is more difficult to model. In contrast to the atmosphere, where mass variations are mostly characterized by long wavelengths (>500 km) [*Merriam*, 1992; *Neumeyer et al.*, 2004], changes from small changes in water storage over very short wavelengths (<10 km) can have a large and immediate impact on gravity observations. Numerous investigations have been undertaken to address the effects of local water storage variations on gravity observations. Studies about the influences of local precipitation, soil moisture and groundwater are given by *Mäkinen and Tattari* [1990], *Crossley and Xu* [1998], *Bower and Courtier* [1998], *Peter et al.* [1995], *Kroner* [2001], *Kroner and Jahr* [2006], *Lambert and Beaumont* [1977], *Llubes et al.* [2004], *Hasan et al.* [2006], *Imanishi et al.* [2006], and *Abe et al.* [2006]. The results indicate that the relationship between local gravity variations and water storage depends on very local geologic and hydrologic conditions, e.g., rock porosity, vegetation, evaporation, and runoff rates.

[4] More recently, the relationship between regional longer-period water storage signals, have also been investigated over distances of several 100 km [*van Dam et al.*, 2001; *Crossley et al.*, 2005]. While a large part of the observed seasonal gravity change can be attributed to long-wavelength changes in water storage, the variability in amplitude and phase of the seasonal signal from superconducting gravimeters in Europe, indicates the importance of a significant local component as well [*Boy and Hinderer*, 2006; *Neumeyer et al.*, 2006].

[5] The aim of this paper is to improve our understanding of the dependence of gravity on extremely local changes in soil moisture around the geodynamic station in Membach, Belgium. *Francis et al.* [2004] investigated this issue when

[1]Seismology, Royal Observatory of Belgium, Brussels, Belgium.
[2]Department of Environmental Sciences and Land Use Planning, Université catholique de Louvain, Louvain-la-Neuve, Belgium.
[3]Hydrogeology and Environmental Geology, University of Liège, Liège, Belgium.
[4]Institute of Meteorology and Geophysics, University of Vienna, Vienna, Austria.
[5]European Center for Geodynamics and Seismology and Natural History Museum of Luxembourg, Walferdange, Grand Duchy of Luxembourg.

0148-0227/06/2006JB004405$09.00

they compared seasonal and shorter-term gravity changes at this location with predicted gravity changes from (1) modeled water storage effects ($1^\circ \times 1^\circ$ spatial resolution and monthly temporal resolution [see *van Dam et al.*, 2001]), (2) volume changes in two surface water reservoirs located at 3 and 6 km, respectively, from the gravity site, and (3) local rainfall. They found that the annual to monthly variations in gravity tracked the reservoir changes well, but that gravity changes with higher frequencies could only be explained by local rainfall events (see Francis et al.'s Figure 4). With respect to the water storage model, *Francis et al.* [2004] focused on the annual signal and found that the amplitude of the gravity changes predicted from the model was very comparable to the observed ones in the SG gravity data, but that study did not analyze the result further. On the other hand the authors could not retrieve a reliable relationship between the water level in the reservoirs and the observed changes in gravity. They concluded that the installation of monitoring probes above the gravimeter would help to constrain a relationship between the local water saturation in the ground and gravity change.

[6] We extend the work of *Francis et al.* [2004] by including observations of soil moisture collected above the superconducting gravimeter (SG). Using the inferred water content and a digital elevation model (DEM) spatially discretized into rectangular prisms, the Newtonian mass effect on gravity is estimated. We find that with an improved understanding of the hydrological effects in Membach, we are able to reduce significantly the short-period scatter changes in gravity time series due to rainfall events, as well as the seasonal variations. The removal of seasonal and higher frequency effects from the gravity signal improves our ability to monitor long-term gravity changes induced by tectonics and postglacial rebound in the region.

2. Geophysical Station of Membach

[7] The Membach geophysical station is located in the eastern part of Belgium. The station houses an accelerometer, short-period and broadband seismometers and the superconducting gravimeter, C021. The SG is installed at the end of a 130 m long tunnel excavated in low-porosity argillaceous sandstone. The gravity sensor is 48.5 m below the surface, which is covered by primarily a deciduous forest canopy. Continuous observations have been taken since August 1995.

[8] The fundamental component of a SG consists of a hollow superconducting sphere that levitates in a persistent magnetic field [*Goodkind*, 1999]. An incremental change in gravity induces a vertical displacement of the sphere. A feedback voltage is induced to keep the sphere at a zero position. This feedback voltage is proportional to the gravity change. The SG provides relative gravity measurements and the most common mode of operation is continuously at a fixed location.

[9] Basic processing of the SG data includes editing and correcting for steps, spikes and other instrumental disturbances (e.g., helium fills). The Earth tides, ocean loading and polar motion effects are subsequently removed. The Newtonian and loading atmospheric influences are corrected by using a linear admittance factor of -3.3 μGal/hPa (for details on the corrections, see *Francis et al.* [2004]). The weak SG instrumental drift is controlled using the absolute gravimeter (AG) FG5 202. Unlike the SG, the AG is mobile and measures the gravity at the station many times per year [*Van Camp and Francis*, 2006]. Being a relative meter, the SG C021 is calibrated using the AG. The AG is also used to remove the secular tectonic trend from the data [*Van Camp et al.*, 2005].

[10] Figure 1a shows the SG time series from Membach. First, we observe a possible long-period (order of 20 years) oscillation in the data, possibly due to hydrological effects. Indeed, such a long-period signal can also be observed in the predicted gravity effect calculated using water storage estimate as well as in the reservoir capacities (Figures 1b and 2a, see sections 3 and 4 for details). However, this is to be confirmed when longer time series are available and since we are primarily concerned with seasonal and shorter-period responses to water storage, our results will not be affected by removing this signal. Therefore we fit and removed a sinusoid with a period of 20 years to the SG data (red line in Figure 1a).

[11] Since June 2003 rainfall has been measured in situ with a tipping bucket type rain gauge (Lufft 8353.01). The tipping is counted and integrated in the data logging system at a minute interval, the resolution is 0.1 mm and the calibration is controlled at least yearly. Before 2003 rainfall data were provided by daily measurements taken at the Gileppe dam, 3 km away from the Membach station.

[12] In August 2004, four CS616 soil water content reflectometers from Campbell Scientific™ [*Campbell Scientific*, 2002] were installed in the shallow partially saturated soil, 48 m above the station. These probes observe soil moisture changes once an hour at 30, 45, 50 and 60 cm below soil surface. The CS616 sensors are time domain soil reflectometers (TDR) that measure the apparent dielectric constant of soil. The sensor consists of two stainless steel rods connected to a multivibrator. The rods act as a waveguide. An electromagnetic pulse travels the length of the probe rods and is reflected from the probe ends traveling back to the probe head. The reflection is detected and a new pulse is triggered. The pulsing frequency in free air is about 70 MHz; however, the velocity of the pulse is dependent on the dielectric permittivity of the material surrounding the rods. The dielectric number at a frequency of 1 MHz to 1 GHz is about 1 for air, 3–4 for major soil minerals and 80 for water because the polarization of water molecules takes time. Thus the dielectric number of soil is highly dependent on the volumetric water content (volume of water per volume of soil) in the unsaturated zone, and consequently, the frequency. A data logger measures the probe output period, which is empirically related to volumetric water content using a calibration equation. The resolution of the probes is 0.1% volumetric water content.

[13] Because of the temperature sensitivity of the probes, negative temperature coefficient (NTC) thermistors are installed at the same position of each probe and NTC data are used to apply a temperature correction on measured soil moisture data.

3. Regional Water Storage Effects on Gravity

[14] The residuals from the 20-year cycle are shown in Figure 1b. We observe a very strong annual signal in the

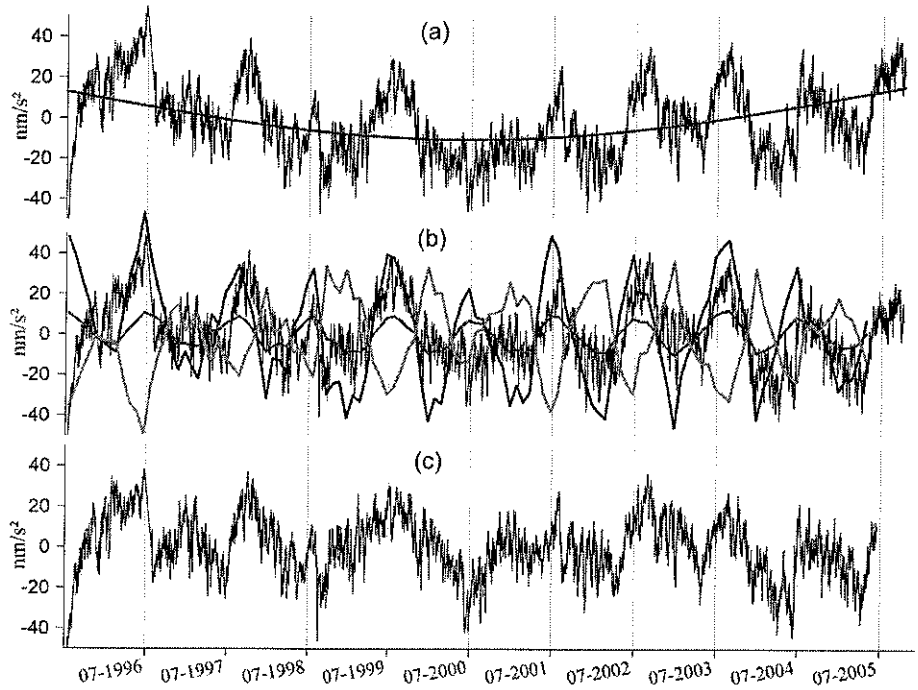

Figure 1. (a) The 10 year time series of SG C021 measurements at the Membach station. For the SG data, the Earth tides, ocean loading, atmospheric, and polar motion effects have been removed. Using AG data, the weak SG C021 instrumental drift was evaluated by fitting an exponential function (drift is -782 exp(-0.085 t) nm s^{-2}, half-life of 8.2 years). The initial exponential decrease from August to December 1995 is due to the SG C021 setup. What remains in these corrected SG residuals, from March 1996 to November 2005, is the uncorrected geophysical signal (hydrological effects and possible crustal deformation due to the postglacial rebound or tectonic activity). The red line is the fitted sinusoid with a period of 20 years. (b) Residuals from the 20-year cycle. The predicted gravity contribution from the water storage estimates has been broken up into its two components: the gravity change arising from the elastic deformation of the Earth (solid red line), and the change arising from the Newtonian mass attraction (blue line, assuming the SG is below the load, and green line, SG above the load). (c) Residuals from the 20-year cycle and after removing the contribution from the elastic deformation of the Earth.

gravity data, which peaks in the late summer/early fall. *Francis et al.* [2004] found that the amplitude of the gravity changes predicted from a regional water storage model, were of the same order of magnitude as the annual signal in the gravity data. The predicted gravity effect calculated using water storage estimates from the *Milly and Shmakin* [2002] Euphrates Land-Energy balance model (1 deg × 1 deg; monthly) is also shown in Figure 1b. The predicted gravity contribution has been broken up into its two components: the gravity change arising from the elastic deformation of the Earth (red line), and the change arising from the mass attraction (blue line if the Newtonian component is computed assuming the gravimeter is below the load, green line if above).

[15] For both components, we observe that the predicted gravity effects are far from perfect. In fact, the gravity model completely misses the gravity low in the summer of 2000. We also observe that the change in gravity due to the elastic deformation, tracks the phase of the observed changes in gravity better than the Newtonian attraction component. This result derives from the fact that the elastic gravity effect is driven by long-wavelength loads, which are accurately represented the water storage model. We find that we are able to reduce the scatter in the gravity residuals from 15.5 to 13.9 nm s^{-2} using the predicted elastic gravity effect. The residuals are shown in Figure 1c.

[16] An annual signal persists in the SG observations, which have been corrected for the regional deformation due to the water storage load. In addition to the seasonal signal, significant short-period variability also exists in the time series. Using the regional water storage model described above, we compute the Newtonian component of gravity. When we remove the mass model effect from the observations, the scatter on the gravity increases from 15.4 to 20.8 nm s^{-2}. This is even worse if one considers that the SG is above the load (green line on Figure 1b). The correlation between local hydrological changes (e.g., soil moisture, well data and rainfall) and gravity indicates that the Newtonian mass component should be determined using local mass change data, which is in accordance with the

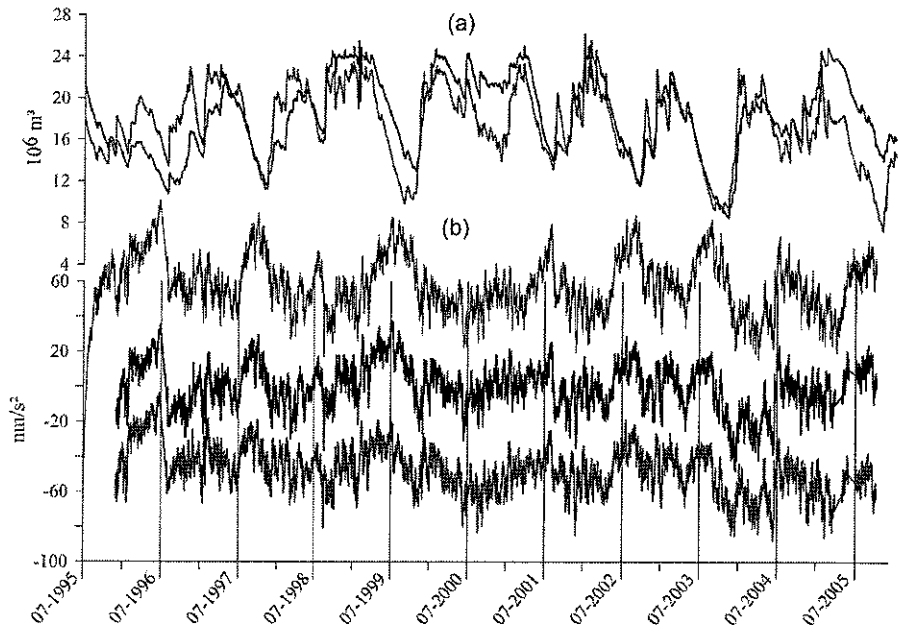

Figure 2. (a) Capacities of the Gileppe (blue) and Vesdre (red) reservoirs 3 and 6 km, respectively, away from Membach. (b) Gravity residuals (same as Figure 1b) before (black) and after fitting the Gileppe (blue) and the Vesdre capacities (red).

publications mentioned in the introduction. To determine the influence of local water mass changes on the SG observations, we have measurements of the level changes in two nearby reservoirs (since 1995), rainfall records (since 2003 at the station, since 1995 at the closest reservoir), and most recently soil moisture measurements.

4. Reservoir Level Changes and Rainfall Effects on Gravity

[17] *Francis et al.* [2004] found that a decrease of 1 m in water level in the nearby reservoirs correlated with a 2.3 nm s^{-2} increase in gravity using only 5 years of data. Using the current 9 year data set, we find that the regression between gravity and water level is -2.2 and -2.6 nm s^{-2} m^{-3} for the Gileppe and Vesdre reservoirs located at a distance of 3 and 6 km from the SG, respectively (Figure 2a). The correlation between the gravity and the water level in both dams is on the order of -0.6. This good correlation is not due to the direct influence of the mass of the water in the dams. However, the capacities are related to the rainfall, surface runoff and stream flow. When we scale the gravity by the regression factor, we find that the scatter on the SG data decreases from 15.5 nm s^{-2} to 12.8 and 12.6 nm s^{-2} for the Gileppe and Vesdre reservoirs. Correcting the gravity data using levels in the dams reduces the amplitude of the seasonal signal in the SG data from 9.2 nm s^{-2} to 4.7 and 3.2 nm s^{-2} for the Gileppe and Vesdre reservoirs (Figure 2b).

[18] As with the reservoir data, the effect of rainfall on the SG data was also addressed by *Francis et al.* [2004], who found a good correlation, 0.46, between gravity and rainfall. Using a 9 year data set of daily rainfall (versus the 5 years of *Francis et al.* [2004]) we find that we are able to reduce the scatter on the AG time series from 13.7 nm s^{-2} to between 11.8 and 12.0 nm s^{-2} depending on our choice of recharge and discharge constants. However, this method is unable to model the seasonal variations (the rainfall around Membach is uniformly spread over the entire year).

[19] The reservoir capacities provide only a qualitative view on the ongoing hydrological processes. Moreover the discharges depend on human factors such as river flow regulation or water consumption, and dams can be saturated (e.g., spring 1997 on Figure 2a). To quantify the physical phenomena based on actual facts and measurements, we have undertaken hydrogeological investigations around the gravity station.

5. Soil Moisture Effects on Gravity

5.1. Hydrogeological Investigations

[20] Geological investigations showed that there is no aquifer near the station. The effective porosity for groundwater of the argillaceous sandstone is only the fissured porosity estimated to ~1%, on the basis of laboratory seismic experiments in similar fissured rocks in the Belgian Ardenne. The saturated hydraulic conductivity is very weak, between 10^{-11} and 10^{-8} m s^{-1} [*Fetter*, 2001]. As a consequence, attempts to establish water catchments in the vicinity of the station were abandoned and drinking water is only provided by two dammed reservoirs of surface water around Membach [*Francis et al.*, 2004]. We have observed a nearly instantaneous response of gravity to rainfall (from 5 nm s^{-2} in 120 min to 40 nm s^{-2} in 120 hours). The low hydraulic conductivity cannot explain the nearly instantaneous response of gravity to rainfall. The cause is rather the

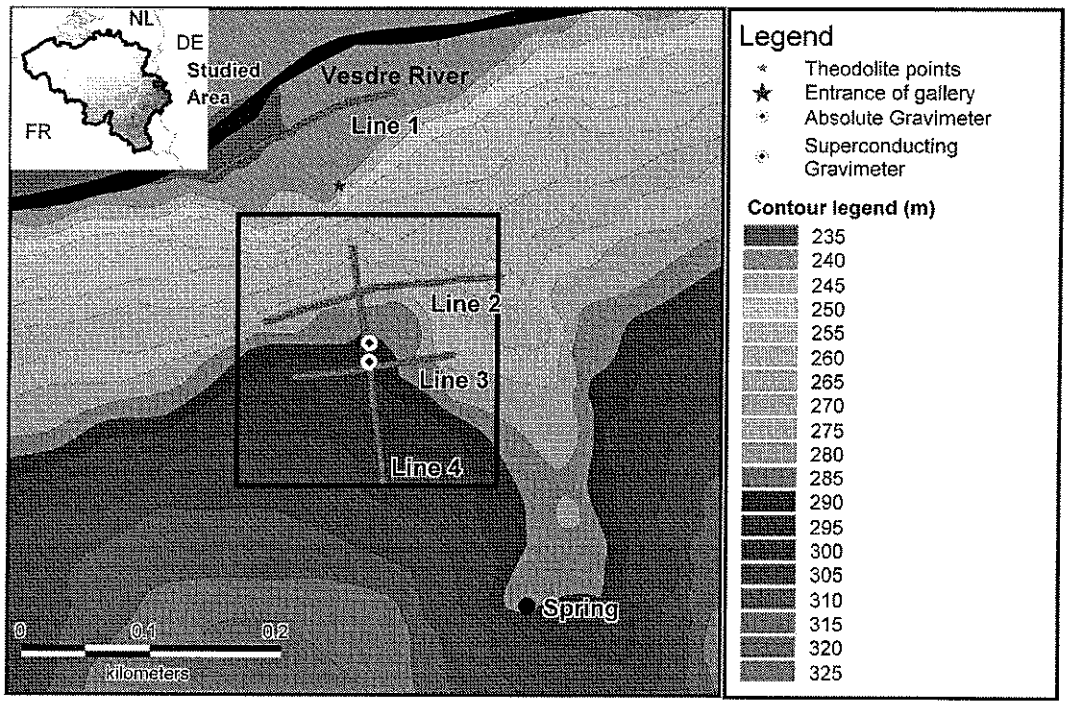

Figure 3. Topography around the station of Membach. The square represents the zone where the 13 seismic refraction profiles were performed above the station, and the aligned green dots correspond to the 4 geoelectric tomography lines. Lines 1, 2, and 4, 96 electrodes; electrode spacing 2.0 m, total length of profile 190 m; line 3, 64 electrodes. Electrode spacing 2.0 m, total length of profile 126 m. Dates, line 1, 6 May 2002; lines 2 and 3, 7 May 2002; line 4, 8 May 2002.

porous weathered layer of rock covering the bedrock where the SG is installed.

5.2. Local Petrology

[21] To determine the thickness of this weathered layer, we first performed four electrical tomography profiles in front of and above the Membach station on 6–8 May 2002 (Figure 3). Results are on Figure 4 for lines 1 and 4. The profiles were measured with the Abem Terrameter SAS 1000 and electrode selector ES 464, four cables with each 16 takeouts and 64 electrodes. For all the profiles we used the Wenner-Schlumberger array [*Pazdirek and Blaha*, 1996] which has a relatively good sensitivity to both horizontal and vertical structures. We designed a measuring protocol with a redundancy of shallow data levels. We used an electrode spacing of 2.0 m. The penetration depth is about 13 m with this array and electrode spacing.

[22] The thickness of the weathered zone covering the bedrock is observed to vary between 0 and 10 m. Surprising enough, the shallow unconsolidated layer has a higher resistivity (1000 to 10,000 ohm m) than the deeper bedrock. This is most likely due to the high porosity of the upper layer coupled with particularly dry weather conditions when the measurements were done. On the other hand, the lower than normal resistivity of the bedrock, can be explained by the presence of clay in the sandstone. The bedrock resistivity is also lower in the valley (~100–200 ohm m, line 1 in front of the station) than on the hill (~500 ohm m, lines 2–4). This regional variation in resistivity can be due to either different clay content in the surface layer, or to more water filled cracks in the bedrock in the valley.

[23] To obtain a more detailed three-dimensional (3-D) model of the unconsolidated layer, 13 seismic refraction profiles were performed in 2005 within a radius of 100 m around the benchmark above the gravimeter. The profiles evidenced a first layer where the P wave velocities average 421 m s^{-1}, with 281 and 647 m s^{-1} as minimum and maximum. The thickness averages 3.4 m with a minimum of 1 m and a maximum of 8 m. In the bedrock, the P velocities average 1526 m s^{-1} with 772 and 3234 m s^{-1} as minimum and maximum. Five of these thirteen profiles

Figure 4. Geoelectric tomography results using the Wenner-Schlumberger method, normal inversion. Uniform logarithmic color scale in ohm meters. Profiles were performed along line 1 in the valley along the river and along line 4, above the station (see Figure 3). Two layers can be distinguished: an upper porous unconsolidated one covering fissured bedrock (low-porosity argillaceous sandstone). These results were confirmed and completed by 13 seismic refraction profiles. The lower resistivity of the bedrock is probably due to the clay content. The higher resistivity in the shallow unconsolidated soil is probably due to high porosity during dry conditions.

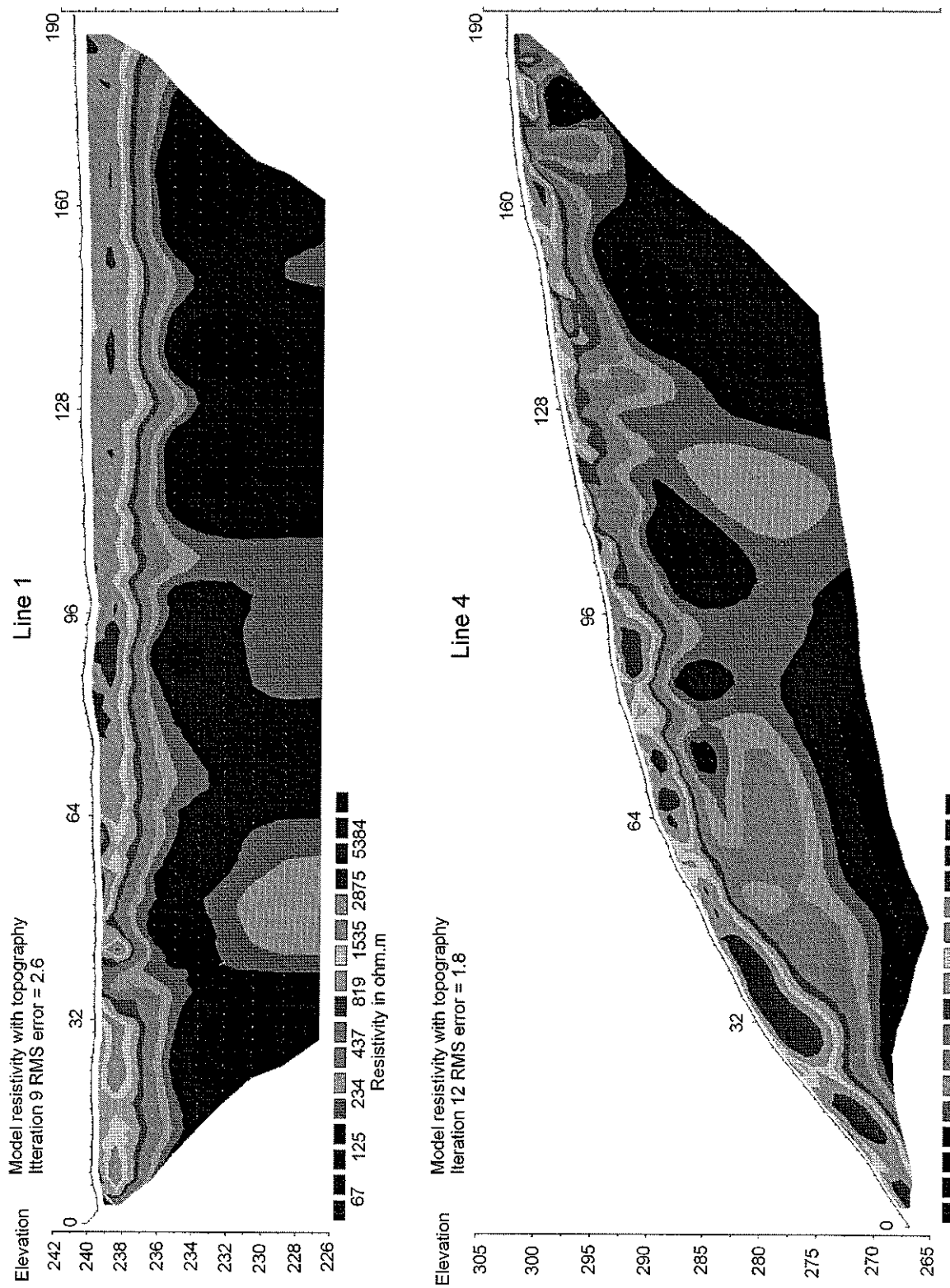
Line 1
Model resistivity with topography
Itteration 9 RMS error = 2.6
Elevation
242
240
238
236
234
232
230
228
226
0
32
64
96
128
160
190
67 125 234 437 819 1535 2875 5384
Resistivity in ohm.m
Line 4
Model resistivity with topography
Iteration 12 RMS error = 1.8
Elevation
305
300
295
290
285
280
275
270
265
0
32
64
96
128
160
190
238 389 638 1045 1713 2806 4599 7536
Resistivity in ohm.m

Figure 4

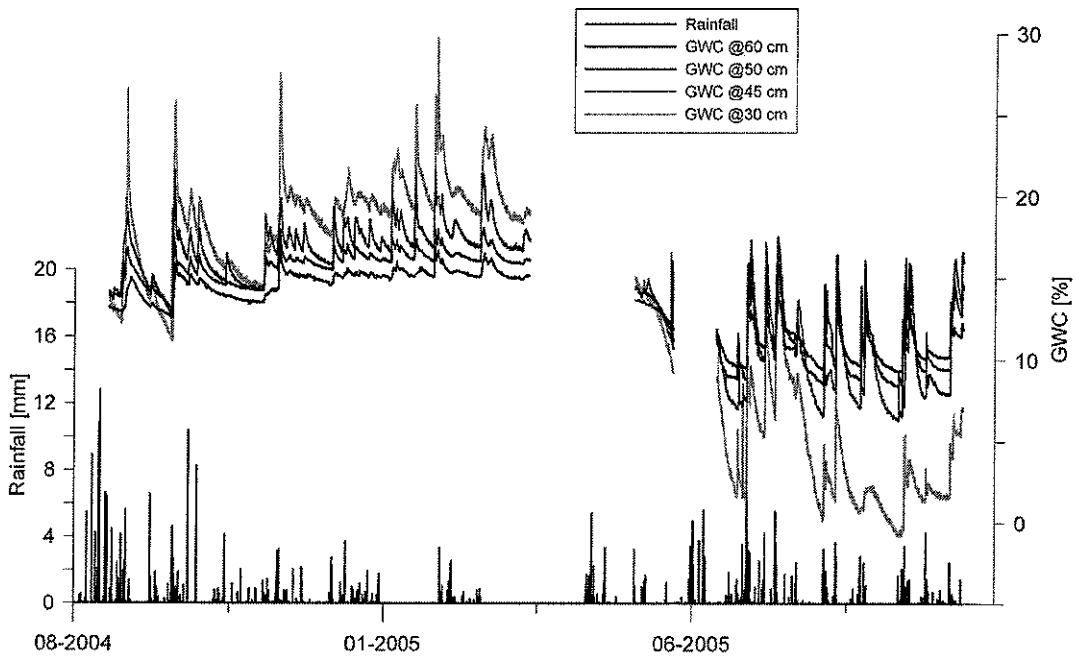

Figure 5. Gravimetric water content inferred from the calibrated reflectometers. In 2005, the gaps in April–May and June–July are due to a dysfunction of the data logger. The precipitation is also indicated (with gaps in January and March–April 2005).

indicated a third layer (2200 to 5222 m s^{-1}) at depths of 6 to 12 m that could indicate the contact between more and less altered bedrock.

[24] The weathered zone consists of a silty soil combined with sandstone blocks and gravels. A granulometric analysis was performed at two sites on the slope above the gravimetry station. At one site the survey found that 53% of the mass consisted of rock fragments greater than 31 mm in diameter and only 27% at the second site. The block content increases with depth, such that hand digging or coring became impossible after 1 m.

5.3. Soil Moisture Observations

[25] The variation of the content of water in the soil was measured using soil moisture probes. Calibration equations are provided with the instruments. These equations, however, are valid primarily for nonstony agricultural soils, by taking the dielectric number and volume fractions of the soil components into account [e.g., *Jacobsen and Schjonning*, 1995]. However, the stone content, the presence of organic matter and clay in the forest soil of Membach can affect strongly the response of the probes, making the equations invalid. We therefore chose to undertake a site-specific in situ calibration of the probes.

[26] We determined the gravimetric soil moisture content by weighing soil samples before and after oven drying. The samples, of about 0.2 dm^3, were taken at three different depths: from 20 to 30 cm, from 40 to 50 cm and from 60 to 70 cm; all at 10 m away from the probes. To limit the sample size, we did not sample rock fragments larger than 31 mm and assumed their water content to be constant in the analysis, although they may also influence the response of the probes.

[27] To measure the gravimetric water content (GWC, mass of water per unit mass of dry soil), sampling was performed 12 times between February and July 2005. Because of a data acquisition problem, reflectometer data were not available in April, May, end of June and beginning of July. However, the 5 remaining pairs of reflectometer measurements and reference GWC were measured within the range 10–25% GWC, corresponding to dry and wet periods. The calibrated measurements are shown in Figure 5.

[28] A linear calibration was derived, providing a relationship between the frequency measured by the soil moisture probes and the GWC. This is a reasonable hypothesis as the bulk density gradient is small in the first top 60 cm. Because of the small number of measurements, no quadratic form was calculated. According to Campbell Scientific™, the linear calibration is within ±1.25% of the quadratic with underestimation of water content at the wet (>40% of volumetric water content (VWC)) and dry ends (<10% VWC) of the soil moisture range. It overestimates the value by up to about 1.2% VWC at about 20% VWC. This is negligible given the other sources of uncertainties, especially the block content as discussed here above.

5.4. Modeling the Gravitational Effect

[29] Using a digital elevation model (DEM) and the thickness of the weathered zone determined by the geophysical investigations, the porous weathered ground layer was discretized in 1600 5 × 5 m rectangular prisms on a 200 × 200 m zone above the gravimeter. The gravitational

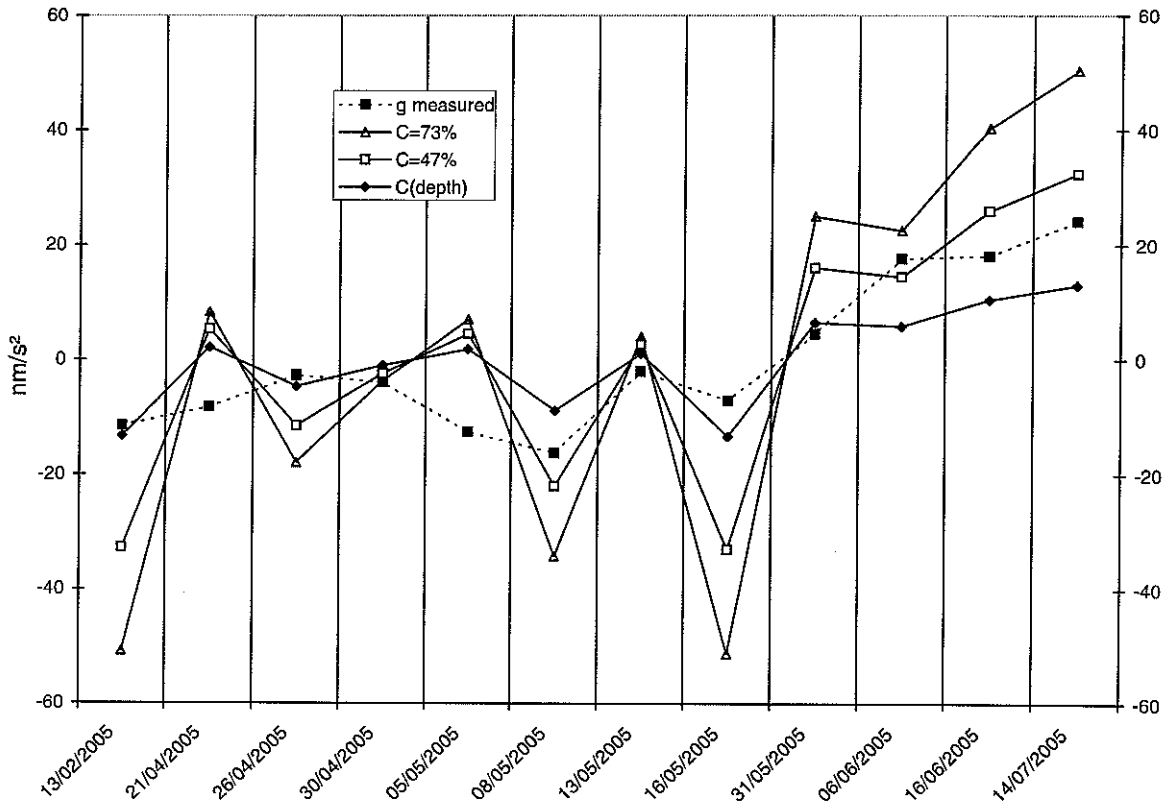

Figure 6. Comparison between the modeled gravitational effect and the observed one for different percentages C of particles smaller than 31 mm in diameter: $C = 73\%$; $C = 47\%$ and C as a function of depth (C, Table 1). The modeled gravitational effect was calculated using the 12 GWC values determined directly from soil sampling. The standard deviation of the difference [observed−modeled] decreases from 2.59 ($C = 73\%$) to 1.54 ($C = 47\%$) and to 0.91 (C function of depth $C(d)$ = 50-20-10-5-5-5-5, compare Table 1).

attraction of each prism was calculated according to [*Banerjee and Das Gupta*, 1977]

$$G\rho_{wet}\int_{x_1}^{x_2}\int_{y_1}^{y_2}\int_{z_1}^{z_2}\frac{zdxdydz}{(x^2+y^2+z^2)^{3/2}}$$

where G is the gravitational constant, and the triple integral integrates over the volume of the rectangular prism delimited by the $x_1y_1z_1$ and $x_2y_2z_2$ coordinates. The density of the wet component of the weathered surface zone is given by

$$\rho_{wet} = \frac{M_{\text{dry}}(1+\Theta_g/100)}{V} = \rho_{\text{bulk}}(1+\Theta_g/100) \qquad (1)$$

where V is the total volume of sample, M_{dry} is the dry mass,

$$\Theta_g = \frac{M_{\text{water}}}{M_{\text{dry}}}100 \qquad (2)$$

is the GWC measured by the recalibrated reflectometers, and

$$\rho_{\text{bulk}} = \frac{M_{\text{dry}}}{V} = 1470\ \text{kg/m}^3 \qquad (3)$$

is the bulk density. To determine the bulk density, 12 dm^3 of ground were excavated 10 m away from the soil moisture probes, from 30 to 60 cm under the surface. Bulk density was then calculated as the oven dry soil weight divided by the sample volume.

[30] Assuming that the density of the rock fragments with diameter greater than 31 mm is constant,

$$\Theta_{g<31} = \frac{M_{\text{wet}}}{M_{\text{dry}}C/100} \Leftrightarrow \Theta_g = \Theta_{g<31}\frac{C}{100} \qquad (4)$$

where C is the mass percentage of particles smaller than 31 mm in diameter and M_{wet} the mass of the wet soil sample. Then equation (1) becomes

$$\rho_{\text{wet}} = \rho_{\text{bulk}}\left(1+\frac{\frac{C}{100}\Theta_{g<31}}{100}\right) \qquad (5)$$

Table 1. Percentage of Particles Smaller Than 31 mm in Diameter C as a Function of Depth and Average of This Percentage as a Function of the Thickness of the Prism[a]

Depth d, m	Percent of Cells	$C(d)$ (C at Depth d), %	Thickness of the Prism, m	C Assigned to the Prism, %
$0 < d < 1$	35	50	<1	50.0
$1 < d < 2$	7	20	<2	35.0
$2 < d < 3$	13	10	<3	26.7
$3 < d < 4$	14	5	<4	21.2
$4 < d < 5$	12	5	<5	18.0
$5 < d < 6$	9	5	<6	15.8
$d > 6$	10	5	>6	14.3

[a]The relative number of cells per thickness is also indicated. The total number of cells is 1600.

In this study, the GWC is the average of the four GWC measurements provided by the four probes. This is a reasonable choice given the high heterogeneity of the soil observed in this forested area.

5.5. Calibration of the Model: Determining the Block Content

[31] Recall that the seismic investigations indicated that the weathered zone can reach a thickness of 8 m and that the block content, which was highly variable, increases with depth. The mass percentage of particles smaller than 31 mm in diameter, C, was estimated by comparing the modeled and observed gravity values. Because of the uncertainties on the in situ calibration of the probes, we used the 12 GWC values determined from soil sampling. Then the gravity effect was computed by considering $C = 73\%$ and $C = 47\%$. In both cases the modeled gravity change overestimated the observed change by 100% and 28%, respectively (Figure 6). As the block content increases with depth d, a more realistic function $C(d)$ must be used.

[32] A seven-layer stratified representation of the soil was considered. The values assigned for $C(d)$ in each layer are given in Table 1. The first six layers are each 1 m in thickness. The final layer reaches a thickness of 2 m in only a few cases and is in general assigned a thickness of 1 m. Because our model can consider only one layer, for each

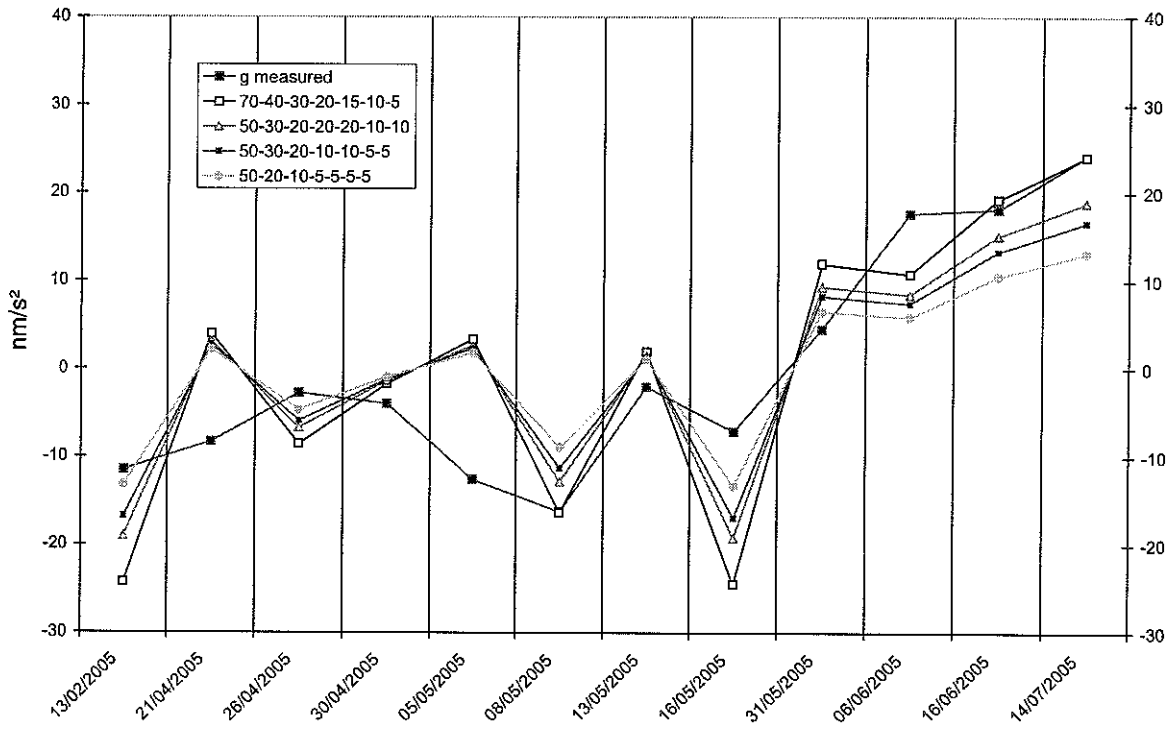

Figure 7. Same as Figure 6 for different functions $C(d)$. The standard deviation of the difference [observed−modeled] decreases from 1.31 ($C(d)$ = 70-50-40-30-15-10-10) to 1.15 ($C(d)$ = 70-40-30-20-15-10-5); 0.98 ($C(d)$ = 50-30-20-20-20-10-10); 0.94 ($C(d)$ = 50-30-20-10-10-5-5) and to 0.91 ($C(d)$ = 50-20-10-5-5-5-5).

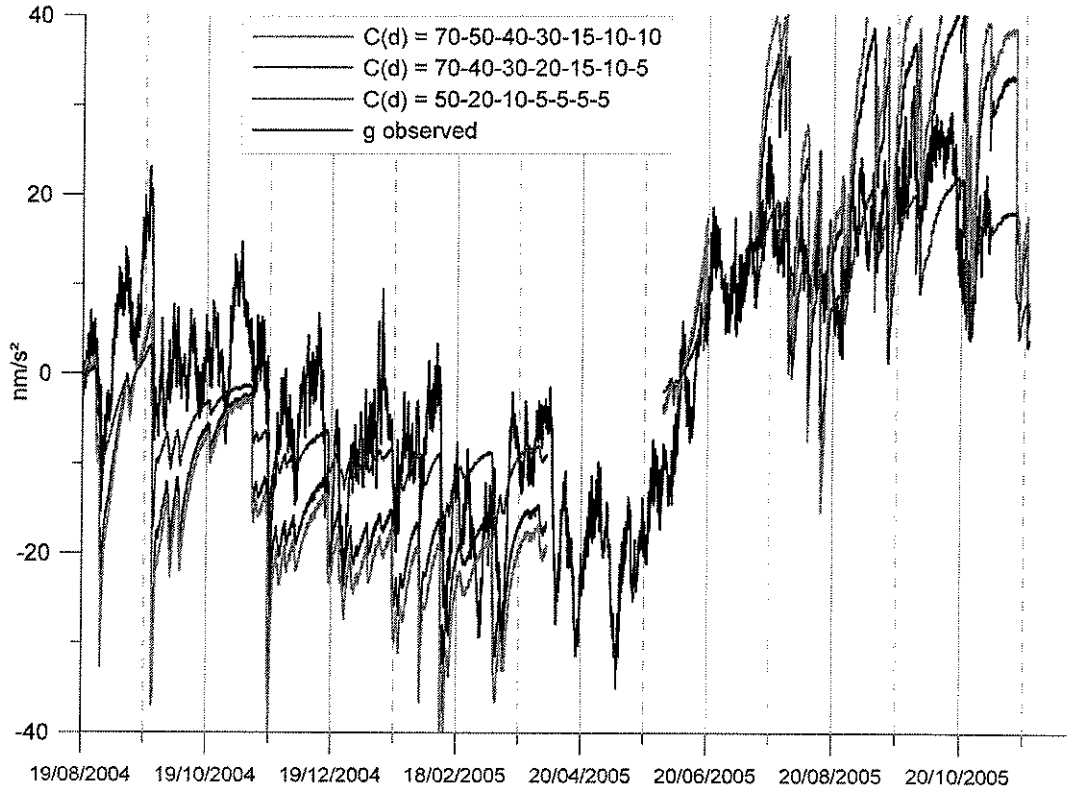

Figure 8. Observed and modeled gravity data for different block content profiles $C(d)$: 70-50-40-30-15-10-10, 70-40-30-20-15-10-5 and 50-20-10-5-5-5-5. The 50-20-10-5-5-5-5 profile provides the best correction, for a bulk density of 1470 kg m^{-3}. The other ones overestimate the hydrological influence.

prism we averaged the values of C in each contributing layers. For example, if the prism is 3 m thick, the assigned value of C = (50% + 20% + 10%)/3 = 26.7%.

[33] The stratified representation of the soil improved the gravity model significantly (Figure 6). The standard deviation of the residuals between the observed and predicted gravity changes decreased from 2.59 (C = 73%) when C was considered to be constant to 1.54 (C = 47%) and to 0.91 when C was allowed to vary as a function of depth, as indicated in Table 1.

5.6. Sensitivity of the Gravity to the Block Content and the Bulk Density

[34] Different block contents have been tested. Some of the results are shown in Figure 7 for different values of $C(d)$. The combination 70-40-30-20-15-10-5 and especially 70-50-40-30-15-10-10 overestimate the short-period variations, while also poorly accounting for the seasonal variation. The other combinations provide similar results, but the standard deviation between the observed and modeled data is minimized for the 50-20-10-5-5-5-5 combination. Applying these cases on the complete time series confirms these results (Figure 8). The correlation coefficient between modeled (red line in Figure 8) and observed gravity changes (black line in Figure 8) is 0.9. More seasons will be necessary to discriminate between these models, but these results indicate already that the consideration of a quickly decreasing porosity with depth corroborates with observed gravity measurements. The model prediction depends on the bulk density; however using densities of 1270 or 1570 kg m^{-3} in place of 1470 kg m^{-3} induces negligible differences.

6. Correcting the Gravity Time Series

[35] Using the in situ calibration of the humidity probes, the best model of depth-dependent block content ($C(d)$ = 50-20-10-5-5-5-5) and the soil moisture time series, the influence of the water content on gravity was calculated. The results are shown on Figure 9 using hourly uncorrected (blue line, before applying the hydrogeological model of depth-dependent block content) and corrected (black line) SG observations. The model accounts for the fast and large gravity variations induced by strong rainfall. For example, on 22–23 September 2004 rainfall (47 mm in 28 h) induced an increase from 12 to 25% in the GWC. The observed gravity decreased by 27 nm s^{-2} and the predicted gravity by 20 nm s^{-2}. The model is particularly successful at reducing the seasonal variation from 15.0 nm s^{-2} to a negligible level of 0.3 nm s^{-2}. More generally, the scatter on the SG data decreases from 13.9 to 6.7 nm s^{-2}.

[36] The model tends to lower the GWC gravity effect when the soil approaches saturation, and to overestimate it

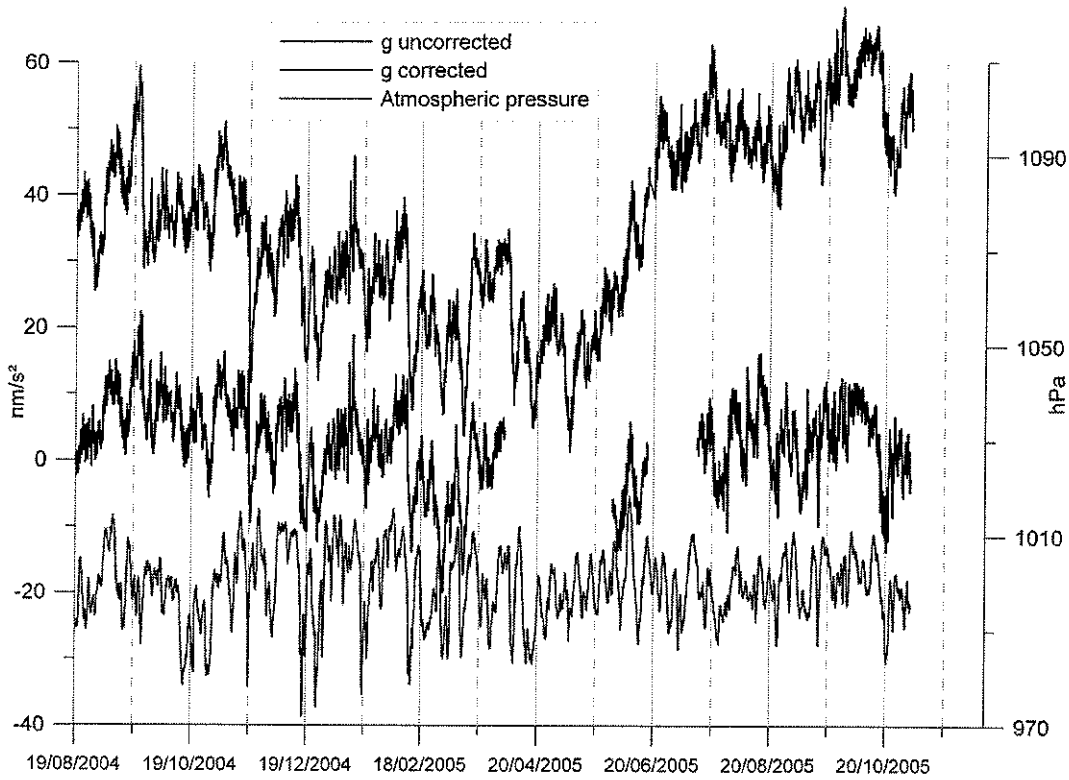

Figure 9. Observed gravity before (blue) and after (black) correction of the modeled effect. Although some short variations are smoothed especially when the GWC is high, the model is especially successful for removing the seasonal variation. Some remaining variations are correlated with the atmospheric pressure (red).

in unsaturated circumstances like the dry summer 2005. This can by explained by the hydraulic conductivity, which depends to some extent on the degree of saturation. On Figure 5, one can also see a threshold effect between the soil moisture and the rainfall: a cumulative rainfall of about 4 mm within a few hours is necessary to induce a noticeable effect on every probe. More reliable corrections of the short-term variations, based on rainfall data, are discussed by B. Meurers et al. (Correcting gravity time series using rainfall modeling at the Vienna and Membach stations and application to Earth tide analysis, submitted to *Journal of Geodesy*, 2006, hereinafter referred to as Meurers et al., submitted manuscript, 2006), who determined a rainfall admittance of -0.386 nm s^{-2} mm^{-1}. They reported on cumulative rainfalls of about 1.5 mm during a dozen of minutes, which induce observable gravity change. However, typical short-term variations on the SG time series, even in dry conditions, are typically of 5–10 nm s^{-2} within a few hours, such that even if applying this admittance improves the SNR, it is difficult to state that every small rainfall systematically induces a directly observable gravity change.

[37] We clearly see a temporal dynamic in the model, which is driven by the desaturation of the soil (i.e., the slow drainage of the soil after a rainfall event is tracked by a slow increase of the modeled gravity) but this specific dynamic is not observed in the actual gravity time series.

[38] An explanation could be that the probes are wrapped with soil, while in the surroundings the water contained in the larger pores between the blocks drains off rapidly.

7. Discussion

[39] The main simplifications in our model are related to the support volume of the soil moisture probes and the hypothesis on the depth-dependent GWC. Indeed, the GWC measurements as determined by the soil moisture probes are, in the model, considered to be representative of the GWC of all prismatic cells in the area. In practice however, variability as measured by means of local-scale soil sensors may be important and the support volumes insufficient to represent effective GWC of a single prismatic cell. Small-scale variability of soil moisture within the prismatic cell may be due to (1) variable water input, driven by rainfall variability, or variability of plant interception or (2) variable water output, driven by the variability of evapotranspiration and soil water drainage. Important small-scale variability of soil hydrological fluxes have been reported for evapotranspiration and root water uptake by *Hupet and Vanclooster* [2002, 2005], for precipitation and plant interception by *Parkin and Codling* [1990]; for drainage by *Mallants et al.* [1996]. This variability is expected to be even more pronounced in forest soils.

[40] In addition to the small-scale variability of the GWC within the prismatic cells, large-scale variability between

the cells may also occur. The 4 ha hydrological catchment supposed to influence the SG measurements within the present model is situated along a hillslope and important larger-scale variability of the topsoil hydrologic attributes is expected to occur. A detailed map of the large-scale variability of the hydrological properties within the considered catchment was not available and could not be further exploited to study the impact of variability on modeling results. In addition to the uncertainty of important variability sources of soil moisture in the horizontal direction, little is known about the depth distribution of soil moisture at the considered site. No measurements greater than 60 cm in depth could be made. Neutron probes could sample larger volumes and provide measurements of the density. Unfortunately, they are difficult to implement, as they must be installed deeper in the ground and require special authorization for using radioelements. This procedure was not feasible at the Membach site.

[41] The remaining observed-modeled gravity residuals are also partly due to improper correction of atmospheric pressure variations. The barometric admittance is the transfer function between gravity and pressure at a single station. This local correction characterizes the gravity signal from the local zone very well (50 km around the gravimeter) [*Merriam*, 1992]. Except during extreme atmospheric conditions, where the Newtonian effect of vertical air mass redistribution (vertical density variation without surface pressure changes) also plays an essential role [*Simon*, 2002; Meurers et al., submitted manuscript, 2006], the precision of this local correction matches the nm s^{-2} level. The regional zone (50 to 1000 km) has a pressure field which usually correlates with the local pressure but will sometimes induce a gravity signal up to 10 nm s^{-2}. Seasonal variation of the vertical density within the atmosphere due to warming and cooling can cause uncorrected gravity variations of about 5–10 nm s^{-2} [*Merriam*, 1992; *Zerbini et al.*, 2001]. Finally, there is also the issue of the variation in the seasonal admittance due to variations in the correlation length of the atmosphere, i.e., the spatial correlation is larger in the winter than in the summer [*van Dam and Francis*, 1998]. A way to improve the correction of the long-period atmospheric pressure effects will be to apply the 3-D model developed by *Neumeyer et al.* [2004].

[42] With these caveats in mind, we have demonstrated that the soil moisture probes provide useful information regarding the dynamics of the water charge and discharge processes above the gravity station, allowing us to remove a large part of the seasonal and shorter-period variations observed in the SG time series at the Membach station.

8. Conclusions and Perspectives

[43] The influence of soil moisture on gravity measurements has been quantified at the Membach station. On the basis of the gravimetric water content measurements and on the spatial discretization of the weathered rock layer in rectangular prisms, the total gravitational effect of the prisms was calculated. The seasonal variations, as well as shorter-period decreases in gravity due to rainfall, were successfully modeled. Because of the absence of a significant aquifer in Membach, we determined that the gravity measurements here are mostly influenced by the saturation rate in the unsaturated surface zone.

[44] This experiment indicates that, while a significant regional water storage signal exists in the SG time series, only detailed geological and geophysical investigations combined with detailed environmental time series, will allow us to model the mass induced gravity changes.

[45] **Acknowledgments.** We are grateful to M. Hendrickx, S. Castelein, M. De Knijf, and G. Rapagnani, who participate in the maintenance of the Membach station, and to K. Vanneste, A. El Bouch, and P. Illing for their help during the geophysical profiles. We thank J. Morren (GmE) and G. Rentmeester for their help in installing the TDR probes and the foresters M. M. Colleau and Delclissar for allowing us to perform this experiment. F. Boulvain is acknowledged for his participation in the geological investigation, and C. Schroeder is acknowledged for his help in the modeling of the Newtonian effects. The rain gauge was tested with the help of Marc Vandiepenbeeck (Royal Meteorological Institute). His great experience on the Belgian climate was also mostly appreciated. Useful hydrological data were also provided by J. Heuschling, J. Huveneers, and R. Grosjean (Direction des Barrages de l'Est - D241). The work benefited from valuable reviews by C. Kroner and L. Timmen.

References

Abe, M., S. Takemoto, Y. Fukuda, T. Higashia, Y. Imanishi, S. Iwano, S. Ogasawara, Y. Kobayashi, S. Dwipa, and D. Sury Kusuma (2006), Hydrological effects on the superconducting gravimeter observation in Bandung, *J. Geodyn.*, *41*(1–3), 288–295.

Banerjee, B., and S. P. Das Gupta (1977), Gravitational attraction of rectangular parallelepiped, *Geophysics*, *42*, 1053–1055.

Bower, D. R., and N. Courtier (1998), Precipitation effects on gravity measurements at the Canadian absolute gravity site, *Phys. Earth Planet. Inter.*, *106*, 353–369.

Boy, J.-P., and J. Hinderer (2006), Study of the seasonal gravity signal in superconducting gravimeter data, *J. Geodyn.*, *41*, 227–233.

Boy, J.-P., J. Hinderer, and P. Gegout (2002), Reduction of surface gravity data from global atmospheric pressure loading, *Geophys. J. Int.*, *149*, 534–545.

Campbell Scientific (2002), *CS616 & CS625 Water Content Reflectometers*, Loughborough, U. K.

Crossley, D. J., and S. Xu (1998), Analysis of superconducting gravimeter data from Table Mountain, Colorado, *Geophys. J. Int.*, *135*, 835–844.

Crossley, D., J. Hinderer, and J.-P. Boy (2005), Time variation of the European gravity field from superconducting gravimeters, *Geophys. J. Int.*, *161*, 257–264.

Fetter, C. W. (2001), *Applied Hydrogeology*, 4th ed., 598 pp., Prentice-Hall, Upper Saddle River, N. J.

Francis, O., M. Van Camp, T. van Dam, R. Warnant, and M. Hendrickx (2004), Indication of the uplift of the Ardenne in long term gravity variations in Membach (Belgium), *Geophys. J. Int.*, *158*(1), 346–352.

Goodkind, J. M. (1999), The superconducting gravimeter, *Rev. Sci. Instrum.*, *70*(11), 4131–4152.

Hasan, S., P. A. Troch, J. Boll, and C. Kroner (2006), Modeling the hydrological effect on local gravity at Moxa, Germany, *J. Hydromet.*, *7*(3), 346–354.

Hinderer, J., and D. Crossley (2000), Time variations in gravity and inferences of the Earth's structure and dynamics, *Surv. Geophys.*, *21*, 1–45.

Hupet, F., and M. Vanclooster (2002), Intraseasonal dynamics of soil moisture variability within a small agricultural maize cropped field, *J. Hydrol.*, *261*, 86–101.

Hupet, F., and M. Vanclooster (2005), Micro-variability of hydrological processes at the maize row scale: Implication for soil water content measurements and evapotranspiration estimates, *J. Hydrol.*, *303*, 247–270.

Imanishi, Y., K. Kokubo, and H. Tatehata (2006), Effect of underground water on gravity observation at Matsushiro, Japan, *J. Geodyn.*, *41*(1–3), 221–226.

Jacobsen, O. H., and P. Schjonning (1995), Comparison of TDR calibration functions for soil water determination, in *Proceedings of the Symposium: Time-Domain Reflectometry Applications in Soil Science*, edited by L. W. Petersen and O. H. Jacobsen, pp. 25–33, Dan. Inst. of Plant and Soil Sci., Lyngby, Denmark.

Kroner, C. (2001), Hydrological effects on gravity data of the geodynamic observatory Moxa, *J. Geod. Soc. Jpn.*, *47*(1), 353–358.

Kroner, C., and T. Jahr (2006), Hydrological experiments at Moxa observatory, *J. Geodyn.*, *41*(1–3), 268–275.

Lambert, A., and C. Beaumont (1977), Nano variations in gravity due to seasonal groundwater movements; implications for the gravitational detection of tectonic movements, *J. Geophys. Res.*, *82*, 297–305.

Lambert, A., N. Courtier, G. S. Sasagawa, F. Klopping, D. Winester, T. S. James, and J. O. Liard (2001), New constraints on Laurentide postglacial rebound from absolute gravity measurements, *Geophys. Res. Lett.*, *28*, 2109–2112.

Llubes, M., N. Florsch, J. Hinderer, L. Longuevergne, and M. Amalvict (2004), Local hydrology, the Global Geodynamics Project and CHAMP/GRACE perspective: Some cases studies, *J. Geodyn.*, *38*, 355–374.

Mäkinen, J., and S. Tattari (1990), The influence of variation in subsurface water storage on observed gravity, in *Proceedings of the 11th International Symposium: Earth Tides*, edited by J. Kakkuri, pp. 457–471, Schweitzerbart, Stuttgart, Germany.

Mallants, D., D. Jacques, M. Vanclooster, J. Diels, and J. Feyen (1996), A stochastic approach to simulate water flow in macroporous soil, *Geoderma*, *70*, 234–299.

Merriam, J. B. (1992), Atmospheric pressure and gravity, *Geophys. J. Int.*, *109*, 488–500.

Milly, P. C. D., and A. B. Shmakin (2002), Global modeling of land water and energy balances. Part I. The land dynamics (LaD) model, *J. Hydrometeorol.*, *3*, 283–299.

Neumeyer, J., J. Hagedoorn, J. Leitloff, and T. Schmidt (2004), Gravity reduction with three-dimensional atmospheric pressure data for precise ground gravity measurements, *J. Geodyn.*, *38*, 437–450.

Neumeyer, J., et al. (2006), Combination of temporal gravity variations resulting from superconducting gravimeter (SG) recordings, GRACE satellite observations and global hydrology models, *J. Geod.*, *79*(10–11), 573–585, doi:10.1007/s00190-005-0014-8.

Parkin, T. B., and E. E. Codling (1990), Rainfall distribution under a corn canopy: Implications for managing agrochemicals, *Agron. J.*, *82*, 1166–1169.

Pazdirek, O., and V. Blaha (1996), Examples of resistivity imaging using ME-100 resistivity field acquisition system, paper presented at 58th Conference and Technical Exhibition, Eur. Assoc. of Geosci. and Eng., Amsterdam, Netherlands, 3–7 June.

Peter, G., F. Klopping, and K. A. Berstis (1995), Observing and modeling gravity changes caused by soil moisture and groundwater table variations with superconducting gravimeters in Richmond, Florida, U.S.A., *Cah. Cent. Eur. Geodyn. Seismol.*, *11*, 147–159.

Simon, D. (2002), Modelling of the field of gravity variations induced by the seasonal air mass warming during 1998–2000, *Bul. Inf. Marees Terr.*, *136*, 10,821–10,836.

Spratt, R. S. (1982), Modelling of atmospheric pressure variations on gravity, *Geophys. J. R. Astron. Soc.*, *71*, 173–186.

Van Camp, M., and O. Francis (2006), Is the instrumental drift of superconducting gravimeters a linear or exponential function of time?, *J. Geod.*, in press.

Van Camp, M., S. D. P. Williams, and O. Francis (2005), Uncertainty of absolute gravity measurements, *J. Geophys. Res.*, *110*, B05406, doi:10.1029/2004JB003497.

van Dam, T., and O. Francis (1998), Two years of continuous measurements of tidal and nontidal variations of gravity in Boulder, Colorado, *Geophys. Res. Lett.*, *25*(3), 393–396.

van Dam, T., J. M. Wahr, P. C. D. Milly, and O. Francis (2001), Gravity changes due to continental water storage, *J. Geod. Soc. Jpn.*, *47*, 249–254.

Williams, S. D. P., T. F. Baker, and G. Jeffries (2001), Absolute gravity measurements at UK tide gauges, *Geophys. Res. Lett.*, *28*(12), 2317–2320.

Zerbini, S., B. Richter, M. Negusini, C. Romagnoli, D. Simon, F. Domenichina, and W. Schwahn (2001), Height and gravity variations by continuous GPS, gravity and environmental parameter observations in the southern Po Plain, near Bologna, Italy, *Earth Planet. Sci. Lett.*, *192*, 267–279.

Zerbini, S., G. Cecconi, D. Colombo, F. Matonti, B. Richter, F. Rocca, and T. van Dam (2005), Monitoring natural and anthropogenic subsidence in the northern Adriatic area by space and terrestrial techniques, *Geophys. Res. Abstr.*, *7*, 1607-7962/gra/EGU05-A-03176.

O. Crommen and A. Dassargues, Hydrogeology and Environmental Geology, University of Liège, B52/3 Sart-Tilman, BE-4000 Liège, Belgium.

B. Meurers, Institute of Meteorology and Geophysics, University of Vienna, Althanstraße 14, UZA II, AT-1090 Vienna, Austria.

T. Petermans, M. Van Camp, and K. Verbeeck, Seismology, Royal Observatory of Belgium, Avenue Circulaire, 3, BE-1180 Brussels, Belgium.

M. Vanclooster, Department of Environmental Sciences and Land Use Planning, Université catholique de Louvain, Croix du Sud 2, BP 2, BE-1348 Louvain-la-Neuve, Belgium. (mvc@oma.be)

T. van Dam, European Center for Geodynamics and Seismology and Natural History Museum of Luxembourg, 19 rue Josy Welter, L-7256 Walferdange, Grand-Duchy of Luxembourg.